Published in final edited form as:
Nat Chem. 2023 March ; 15(3): 413–423. doi:10.1038/s41557-022-01094-w.

Dimeric and Trimeric Catenation of Giant Chiral [8+12] Imine Cubes Driven by Weak Supramolecular Interactions

Dr Bahiru Punja Benke, M.Sc,
Tobias Kirschbaum,
Dr Jürgen Graf [Prof],
Dr Jürgen H. Gross,
Dr Michael Mastalerz*
Organisch-Chemisches Institut, Ruprecht-Karls-Universität Heidelberg, Im Neuenheimer Feld 270, 69120 Heidelberg, Germany

Abstract

Mechanically interlocked structures, such as catenanes and rotaxanes, are fascinating synthetic targets and some are used for molecular switches and machines. Today, the vast majority of catenated structures are built upon macrocycles and only a very few examples of three-dimensional shape-persistent organic cages forming such structures are reported. However, the catenation in all these cases was based on a thermodynamically favoured **π-π** stacking under certain reaction conditions. Here, we show that catenane formation can be induced by adding methoxy- or thiomethyl groups to one of the precursors during the synthesis of chiral [8+12] imine cubes, giving dimeric and trimeric catenated organic cages. To elucidate the underlying driving forces, we reacted eleven differently 1,4-substituted benzene dialdehydes with a chiral triamino tribenzotriquinacene under various conditions to study whether monomeric cages or catenated cage dimers are the preferred products. We find that catenation is mainly directed by weak interactions derived from the substituents rather than by **π**-stacking.

Since the first report of Wasserman in the early 1960s of a catenane as a statistical occurring by-product during a macrocyclization via acyloin condensation,[1] the interest in interlocked molecular structures developed rapidly in the last decades,[2,3] especially because such compounds build the fundamental knowledge for supramolecular switches and machines.[4,5,6] Although Lüttringhaus and Schill introduced already rational synthetic approaches towards a number of interlocked structures in the 1960s,[7] the real ignition of

Corresponding author Correspondence to michael.mastalerz@oci.uni-heidelberg.de.

Author Contributions
B.P.B. found the catenation reaction. M.M. and B.P.B. conceived and planned the project. B.P.B. did all the experimental work. M.M. and B.P.B. analysed and interpreted the results. T.K. performed quantumchemical calculations. J.G. was responsible for the NMR experiments, especially in helping elucidating the structure of catenanes. J.G. measured all mass spectra. M.M. and B.P.B. prepared the manuscript, which was edited by all authors.

Competing interests
The authors declare no competing interests.

Europe PMC Funders Author Manuscripts

this research field began with the work by Jean-Pierre Sauvage and coworkers with a high-yielding catenane synthesis exploiting the templated coordination of two molecular strands by a metal ion before closing these to two interlocked macrocycles via Williamson ether synthesis.[8,9] This concept of using a template was and still is the most frequently applied strategy for the synthesis of more complex interlocked structures such as Borromean rings,[10] various knots,[11,12,13,14] a Star of David catenane,[15] poly[n]catenanes,[16] or interlocked coordination cages.[17,18,19,20,21] Besides ligand to metal ion coordination, weaker and less directing supramolecular interactions—such as hydrogen bonding or π-π stacking—have been used to arrange molecular precursors in the right fashion to synthesize interlocked structures.[22]

In contrast to the relative large number and diversity of interlocked coordination cages,[18] there are still only a few examples of purely organic cage catenanes reported to date. The first example was reported by Beer et al.[23] They exploited a template effect of sulfate anions, interacting with carbamate units to prearrange two tripodal precursor molecules in such a way that by the end-capping of these via a copper-mediated 1,3-dipolar cycloaddition a triply interlocked cage dimer was formed in 21% yield. One year later, in 2010, Cooper and coworkers described that by changing conditions for the synthesis of a [4+6] imine cage by adding catalytic amounts of trifluoroacetic acid to the reaction solution in acetonitrile or dichloromethane, these [4+6] imine cages form triply interlocked dimers,[24] which was proven by single-crystal X-ray diffraction. It was suggested that π-π stacking most probably is the driving force for the catenane formation and if a competing aromatic solvent was present in certain amounts, this indeed suppressed the catenane formation. In 2014, the formation of a quadruply interlocked dimer of giant [12+8] boronic ester cage was described,[25] which was clearly characterized by single-crystal X-ray diffraction. The only difference between the interlocked cage dimer and a corresponding monomeric [12+8] boronic ester cage[26] published before is the position and length of solubilizing alkyl-chains in the molecular precursors, which led to the hypothesis that additionally weak dispersion interactions may be responsible for the catenane formation to overcome any entropic penalty. Similar but more distinct, this entropic penalty was balanced by dispersion interactions in the formation of a hydrocarbon cage and its catenated dimer made by alkyne metathesis.[27] Depending on concentration of reacting monomers, the equilibrium between monomeric and interlocked cage could be shifted towards the one or the other metathesis product. The authors assumed that a triply interlocked structure is energetically more favored than a singly one due to a maximization of filled space. 2015, Li et al. exploited the hydrophobic effect to achieve an interlocked cage dimer via a hydrazone bond formation in water.[28] Very recently, the group of Shaodong Zhang presented the formation of a triply interlocked catenane of a [2+3] imine cage.[29,30] Again, it was concluded that the driving force is the energetic benefits of additional π-π stacking. In contrast to the before mentioned examples, here the dimer formation has been studied more detailed by kinetic NMR measurements and time-dependent mass spectrometry; however, no thermodynamic assumptions were corroborated by experiments. It is worth mentioning that Greenaway et al. described the unexpected formation of a bridged cage catenane, during large high-throughput screening.[31]

During our ongoing work on using chiral triamino tribenzotriquinacenes (TBTQs) in the condensation with aromatic aldehydes to study self-sorting of cages,[32,33] we serendipitously found a substituent driven formation of dimeric and trimeric cage catenanes, which is described herein.

Results and Discussion

Synthesis and characterization of cage and catenanes

Inspired by Warmuth's chiral cube,[34] based on the condensation of eight molecules of cyclotriveratrylene (CTV) trisaldehyde and para-phenylene diamine, we intended to use a chiral TBTQ precursor instead, which is in contrast to the CTV structurally fixed and cannot racemise during cage formation. Indeed, the condensation of enantiopure triamino TBTQ (*P*)-**1**[35] with 2,4-dihydroxy terephthalaldehyde **2** under typical conditions we used before for similar systems (cat. TFA, CDCl3 room temperature)[34,36] gave clean chiral [8+12] cage **OH-cube** in 88% isolated yield (Fig. 1) and was identified by NMR and mass spectrometry.

Originally we were interested in post-stabilizing the **OH-cube** by Pinnick-oxidation to turn imine bonds into amide bonds.[37] As reported before, this does not work with the phenolic hydroxy groups present. To avoid a 24-fold post-synthetic Williamson etherification on **OH-cube**,[38] we instead condensed TBTQ (*P*)-**1** with dimethoxy terephthalaldehyde **3** under the same conditions (Fig. 2a). In contrast to the reaction with aldehyde **2**, here the ^{1}H NMR spectrum of the crude product was very complex with a large number of peaks in the aromatic as well as in the aliphatic region (Fig. 2b). The corresponding MALDI-TOF MS revealed that beside the [8+12] **OMe-cube** (*m/z* = 5623.21), a [16+24] condensation product (*m/z* = 11245.46) was generated and even a small peak with *m/z* = 16868.53 was detected (Fig. 2c), suggesting that a larger [24+36] species may have formed. Taking into consideration the complex ^{1}H NMR spectra reported for triply interlocked cages before,[24] it was assumed that these species are most likely catenated dimer **(OMe-cube)$_2$** and trimer **(OMe-cube)$_3$** rather than larger more symmetric and non-interlocked species. By applying recycling gel permeation chromatography (r-GPC) with dichloromethane as solvent, it was possible to separate the three compounds after multiple cycles (Fig. 2d, and Supplementary Section 8).

As described in literature before, the equilibrium between monomeric and catenated cage shifts towards the latter by increasing the concentration of reactants and vice versa to the monomeric cage by decreasing it. Therefore, the reaction was performed at different concentrations (between 0.42 mM and 42.8 mM) and analyzed mainly by MALDI-TOF MS (Supplementary Table 1). As expected, with higher concentration more catenated compounds **(OMe-cube)$_2$** and **(OMe-cube)$_3$** were found and the concentration needs to be 0.42 mM or below to avoid the formation of those and to form monomeric cage **OMe-cube** exclusively. For comparison; reactions with dihydroxy terephthaldehyde **2** at various concentrations (up to 42.8 mM) did not give any catenated species and in each experiment only monomeric cage **OH-cube** was detected by ^{1}H NMR spectroscopy (Supplementary Fig.398). It is worth mentioning that as soon as a chloroform or dichloromethane solution of monomeric cage **OMe-cube** was concentrated by rotary evaporation (50 °C, reduced

pressure), the equilibrium immediately shifted towards the catenated products **(OMe-cube)$_2$** and **(OMe-cube)$_3$** as found by NMR and r-GPC analysis. On one hand, this clearly demonstrated the dynamic covalent chemistry character and thus thermodynamically driven formation of the catenane.[39] On the other hand, it made the separation and characterization of monomeric cage **OMe-cube** more challenging.

Despite these findings, we were able to develop a synthetic protocol to isolate **OMe-cube** in 85% yield, avoiding long reaction times, certain concentration and temperature thresholds and exploiting the low solubility of the cage in acetonitrile (Supplementary Section 2). To our delight, by changing the solvent to 1,1,2,2 tetrachloroethane (TCE), monomeric cage **OMe-cube** can be synthesized even at higher concentration (5.4 mM), without the necessity of GPC separation, in 76% yield (Fig. 3a). On the other hand, running the reaction of **3** and **1** in dichloromethane instead of CHCl3 at 10.7 mM concentration and 80 °C for 3 days allowed us to push the equilibrium towards the tricatenane **(OMe-cube)$_3$**, which was isolated in 80% yield (Fig. 3a). The best results for the dimeric cage **(OMe-cube)$_2$**, was achieved, when dialdehyde **3** and triamine **1** were reacted at 10.7 mM scale. However, **(OMe-cube)$_2$** still needed to be separated by r-GPC from **OMe-cube** and **(OMe-cube)$_3$** at 35 °C to be obtained in 46% isolated yield (Fig. 3a).

Mechanistic investigation of monomeric cage to dimeric catenane reaction

To get some more mechanistic information of catenane formation, the transformation of **OMe-cube** to **(OMe-cube)$_2$** was studied in more detail. Kinetic NMR experiments indicated that full equilibrium between **OMe cube** ($c0$ = 1.35 mM, CDCl3) and **(OMe-cube)$_2$** was achieved after approx. 800 mins (k_1 = 10.5 ± 0.4 $M^{-1}s^{-1}$), if catalytic amounts of TFA are present (Supplementary Fig. 506). In the absence of acid, no conversion at all was detected even after 24 hrs (Supplementary Fig. 507). By mixing a ^{15}N-labelled cage ***OMe-cube** in a 1:1 stoichiometry with nonlabelled **OMe-cube** under reaction conditions (cat. TFA, CDCl3) and analyzing the mixture after 3 days by TIMS-TOF MS revealed that all units (TBTQ and linkers) are fully scrambling to a statistical mixture, suggesting that during catenane formation all TBTQ units must be disconnected from the cage scaffolds at a certain stage, opening the cages for catenation (Supplementary Figs. 508 & 509).

Structural analysis of cage and dimeric and trimeric catenanes

The GPC purified fractions were again separately injected into r-GPC that shows three distinct peaks each of nearly Gaussian shape with retention times of 25.4 min (1st fraction), 25.9 min (2nd) and 27.7 minutes (3rd) were detected (Figs. 3b, d and f). MALDI-TOF MS analysis of each fraction (Figs. 3c, e, and g) now show single peaks exclusively at m/z = 16868.69 (1st fraction), m/z = 11245.57 (2nd fraction) and m/z = 5623.24 (3rd fraction) which exactly fit to a [24+36], a [16+24] and a [8+12] species. The ^{1}H NMR spectrum (Fig. 3h) of the 3rd fraction was very simple, showing signals comparable to **OH-cube** and in combination with the mass spectrum (Fig. 3c) this compound was clearly identified as the monomeric chiral [8+12] **OMe-cube**. By diffusion-ordered NMR spectroscopy (DOSY) in deuterated dichloromethane at 295 K only one trace was detected with a diffusion coefficient of $D = 3.09 \cdot 10^{-10}$ m^2s^{-1} which corresponds according to the uncorrected Stokes-Einstein equation to a solvodynamic radius of rS = 16.9 Å (Supplementary Fig. 308). In contrast

to the relatively simple ^{1}H NMR spectrum of monomeric **OMe-cube** (Fig. 3h), that of the [16+24] species was much more complex (Fig. 3i). Nevertheless, despite the large number of signals, most of them were sharp and did not superimpose, allowing a more detailed analysis of the structure (Fig. 4a and for detail structural analysis see Supplementary Section 13). By 2D NMR experiments, eight different types of imine-protons and eight different methoxy-protons were identified (Figs. 4b and 4c). This is exactly the number expected for a triply interlocked cage dimer (see cartoon in Fig. 4h.) Other possible catenanes such as a singly interlocked dimer (Fig 4g, twelve imine peaks) or quadruply interlocked dimer (Figure 4i, six imine peaks) can clearly be ruled out. By DOSY NMR in dichloromethane at 295 K only one trace of signals for (**OMe-cube**)$_2$ confirmed that this is a single species. The diffusion coefficient $D = 2.67 \cdot 10^{-10}$ m^{2}s^{-1} corresponds to a solvodynamic radius of 19.6 Å (Supplementary Fig. 309). This is slightly larger than for **OMe-cube** (16.9 Å) which is consistence with its slightly larger size.

The trimeric interlocked cage **(OMe-cube)$_3$** shows at room temperature much less resolved multiple broad peaks in the ^{1}H NMR spectrum (Supplementary Fig. 72) in contrast to dimer **(OMe-cube)$_2$**. However, in toluene-d8 at 375 K a much better resolved spectrum was obtained, showing sets of 12 magnetically different peaks, such as 12 imine protons and 12 signals of the terminal CH_3 group of the propyl chains (Figs 5a-5c, Supplementary Figs. 88- and 89). This excludes a syn-distal connectivity (36 imine peaks; Fig 5c, for models see, Supplementary Fig. 522) as well as a syn-proximal connectivity at two adjacent corners at the central cube (here 72 imine peaks are expected; Fig. 5d, for models see, Supplementary Fig. 523). For both a chain-like anti-connected catenane **(OMe-cube)@(OMe-cube)@(OMe-cube)** as well as for an interwoven catenane [**(OMe-cube)@(OMe-cube)]@(OMe-cube**) the same number—12—of magnetically different peaks are expected, as has been found (for models, see Supplementary Figs. 520 & 521). However, since the trimeric catenane **(OMe-cube)$_3$** is still very soluble under reaction conditions and no traces of larger oligomers such as tetrameric and pentameric cages **(OMe-cube)4** or **(OMe-cube)5** are found by mass spectrometry, it seems to be more likely that the interwoven catenane [**(OMe-cube)@(OMe-cube)]@(OMe-cube**) (Fig. 5a) and not the chainlike anti conformed catenane **(OMe-cube)@(OMe-cube)@(OMe-cube)** (Fig. 5b) has formed. If it would be the latter motif, we would expect at least some formation of longer oligomers, which is not the case. On the other hand, an interwoven tetrameric catenane is simply not possible for steric reasons, which once more would explain the absence of larger species and thus favors this motif for the trimeric catenane [**(OMe-cube)@(OMe-cube)]@(OMe-cube**). DOSY NMR of **(OMe-cube)$_3$** again shows a single trace with a diffusion coefficient $D = 2.64 \cdot 10^{-10}$ m^{2}s^{-1}. The calculated solvodynamic radius of 19.8 Å (Supplementary Fig. 310) was found to be almost similar with the dicatenane **(OMe-cube)$_2$** (19.6 Å) once more suggesting a tightly packed interlocked structure. In DOSY NMR spectra of a 1:1 stoichiometric mixture of pure **(OMe-cube)$_2$** and **OMe-cube)$_3$** (Supplementary Fig. 512) the difference between the diffusion coefficient values is very small further supporting the more dense interwoven catenane [**(OMe-cube)@(OMe-cube)]@(OMe-cube**) model.

It is worth mentioning that for **OH-cube**, **OMe-cube**, **(OMe-cube)$_2$** as well as **(OMe-cube)$_3$** and other cage catenanes described below innumerous large single-crystals from various solvents have been obtained. Unfortunately, even with synchrotron radiation no resolution has been obtained to elucidate the solid-state structures.

Investigation in driving force for catenation

We were interested to get further insight into the driving force of the unique catenation of methoxy cage **OMe-cube** to dimer **(OMe-cube)$_2$** and even to trimer **(OMe-cube)$_3$** and why we do not see any such catenation for the hydroxyl substituted **OH-cube** under any concentration. Due to the triply interlocked catenation of dimer (**OMe-cube)≡OMe-cube)** in favour of a possible singly interlocked dimer (**OMe-cube)-(OMe-cube),** the aforementioned **π-π** stacking as driving force, found for almost all other yet in literature described interlocked organic cages, was excluded (see above), otherwise singly interlocked catenation should have been formed preferably. In addition for **OH-cube** a higher tendency of dimerization would have been expected than for **OMe-cube**, because intramolecular H-bonding of the hydroxyl imine is stiffening the **π**-backbone and strongly enhances intermolecular **π-π** stacking.[40] This assumption is strengthened by the fact that under various reaction conditions (different acid concentration, different concentration of reactants, different solvents, different and elevated temperature, different reaction times (up to several months!)) no substantial catenane formation was found for **OH-cube** (see Supplementary Figs. 398, 400, 401 and 510). A kinetic formation driven by precipitation was also ruled out, because the reaction mixture of **1**, **2** and **OH-cube** were at all times clear solutions.[39] Furthermore, mixing **OH-cube** and ^{15}N labelled ***OH-cube** in a 1:1 ratio and treating this mixture under reaction conditions, shows by TIMS-TOF MS two highest peaks at *m/z* = 5297.56 (corresponding to **OH-cube-^{15}N12)** and at *m/z* = 5320.54 (corresponds to **(OH-cube-^{15}N12+Na)** suggesting a complete scrambling even in solution, supporting the thermodynamically formation of **OH-cube** and that it is not a kinetic trap (Supplementary Figs. 510 &511).[41]

Since **π**-stacking was ruled out as driving force, we first hypothesized that dipole-dipole interactions (so-called Keesom interactions)[42] of the methoxy groups may be responsible for the catenation, as e. g. found in single crystals of methoxy-substituted **π**-systems (d(Me$O\cdots C$H$_3$O) = 3.1 Å).[43] In this respect, it is worth mentioning that the bridged cage catenane reported by Greenaway et al., when originally achieving cages based on dimethoxy terephthaldehyde **3**,[31] could rely on such weak interactions, although a closer look at the X-ray structure show the same methoxy-methoxy interaction motif, albeit with a larger distance between the functional groups of d(Me$O\cdots C$H$_3$O) = 3.5 Å (Supplementary Fig. 513). Conformational analysis by DFT calculations (Supplementary Section 19) of **OMe-cube** as well as NOESY cross peaks between imine CH and the aromatic TBTQ protons revealed a low barrier of rotation of the linker units at room temperature, which is also present in the triply interlocked dimer (**OMe-cube**)$_2$ allowing the mechanically interlocked molecule to adopt conformations that have three such methoxy-methoxy interactions (Fig. 6c). According to this assumption (Supplementary Figs. 513d & e), one methoxy group per dialdehyde unit should be enough to foster catenation and indeed reacting dialdehyde

12 (with only one methoxy group present) with triamine **1** in DCM clearly gave catenated **(H/OMe-cube)$_2$,** as determined by MS (Supplementary Fig. 345).

If methoxy groups are absent, no catenane formation should occur. Thus triamine **1** was reacted with non-substituted terephthalaldehyde **4** (Fig. 6a) under different conditions (various solvents, Supplementary Fig. 405) and no catenane formation was observed. Pure **H-cube** was isolated in 90% from THF. By adding two methyl substituents instead of two methoxy groups to the aldehyde (**5**) still almost no catenane formation is observed by ^{1}H NMR (Supplementary Fig. 406) and monomeric **Me-cube** is formed in 84% yield. As soon as the alkyl substituents at the dialdehyde precursor (**6**) get longer (here ethyl), the possibility of intermolecular dispersion interactions[44] (Fig. 6b) is slightly increased and now some catenane (**Et-cube)$_2$** was found by ^{1}H NMR spectroscopy as well as MS (Supplementary Fig. 407) besides monomeric **Et-cube** (which still is the main product). Comparing the different results of **Me-cube** versus **Et-cube**, based on the simple elongation of the alkyl chains by one methylene unit each, electronic effects to foster π-π-stacking can again be ruled out, because the methyl- as well as the ethyl-substituents have almost the same Hammett parameters (σm(Me) = -0.07; σm(Et) = -0.07; σp(Me) = -0.17; σp(Et) = -0.15).[45] As for **OMe-cube** and **(OMe-cube)$_2$**, the ratio of catenane (**Et-cube)$_2$** versus monomeric cage **Et-cube** was also strongly solvent dependent for the reaction of triamine **1** and aldehyde **6** and in THF the amount of catenane was higher than e.g. in CHCl3 and both compounds (monomer and catenane) were selectivity achieved by adjusting the conditions. The reaction in CHCl3 at room temperature gave monomeric cage **Et-cube** in 75% isolated yields, whereas running the reaction in THF gave after separation 35% of the catenated dimer (**Et-cube)$_2$** in pure form.

To further exclude pure electronic effects for a probable π-stacking, we reacted triamine **1** with diethoxy- and diisopropoxy dialdehydes **7** and **8**, (Fig. 6a) where the substituents have comparable Hammett parameter as in dimethoxy dialdehyde **3** (σm(OMe) = 0.12; σm(OEt) = 0.10; σm(O^{i}Pr) = 0.10), but are of different steric demand. Whereas for the diethoxy dialdehyde **7** some catenane formation of (**OEt-cube)$_2$** was observed, for diisopropoxy dialdehyde **8** no catenane (**OiPr-cube)$_2$** was observed by ^{1}H NMR spectroscopy (Supplementary Figs. 408 & 409), supporting once more the hypothesis that the catenane formation is mainly driven by weak interactions derived from the substituents rather than by π-stacking and in case of the latter steric repulsion is stronger than the weak attraction (Fig. 6b, Charton steric parameter for Me, Et, and ^{i}Pr are νMe = 0.52; νEt = 0.56; νiPr = 0.76).[46]

By increasing these weak interactions, the equilibrium may be shifted towards the interlocked structures. By using dimethylthioether **9** in the condensation with triamine **1** in CDCl3 almost exclusively the triply interlocked catenated dimer **(SMe-cube)$_2$** was formed (Fig. 6a and Supplementary Fig. 410). Harsher conditions were needed to push the system to the trimeric cage **(SMe-cube)$_3$,** which was isolated in 58% yield by using dichloromethane as a solvent in combination with elevated temperature (80 °C, screw-capped vessel, 4 days). By 2D NMR spectroscopy, the same linear and interwoven catenation motif was found as for **(OMe-cube)$_3$** (Supplementary Fig. 495). Switching the solvent system to TCE,

monomeric **SMe-cube** was isolated in 80% yield. Again, to rule out electronic effects based on the thioalkyl substituent donating to the π-system of the aromatic dialdehyde, di-*tert*-butylthioether substituted dialdehyde **10** with two sterically demanding *tert*-butyl groups was investigated in the reaction (νMe = 0.52 vs νtBu = 1.24).[46] As expected, only clean monomeric **SC(CH$_3$)3-cube** was formed and isolated in 75% yield (Supplementary Fig. 411). Finally, we investigated the reaction of dibromo dialdehyde **11** with triamine **1,** to see whether halogen bond formation[47] can also induce catenation. Although the mass spectrum of the reaction mixture in CD_2Cl_2 showed a pronounced peak at m/z = 13591.6, which is the double amount of the monomeric **Br-cube** (m/z = 6796.4), in the correlated ^{1}H NMR spectrum only small detectable peaks of any interlocked species are present besides mainly those signals of pure monomeric **Br-cube** (Supplementary Fig. 412). However, in contrast to all other reactions, here a precipitate was formed of very low solubility, which may contain insoluble **(Br-cube)$_2$**.

Thermodynamic studies

To correlate the weak interactions responsible for catenation, the systems where catenation occurred have been studied by concentration dependent NMR spectroscopy (Supplementary Section 12), to estimate the Gibb's enthalpy of cage to catenane transformation. With $\Delta G298$ = -26.7 kJ/mol the reaction of **2 SMe-cube → (SMe-cube)$_2$** is about 6 kJ/mol higher as for the methoxy cages **2 OMe-cube → (OMe-cube)$_2$**, $\Delta G298$ = -20.8 kJ/ mol) and almost 10 kJ/mol higher than found for the ethoxy cages **2 OEt-cube → (OEt-cube)$_2$**, $\Delta G298$ = -15.7 kJ/mol) (Fig. 6d), Unfortunately, in CDCl3 the amount of **(Et-cube)$_2$** besides **Et-cube** was too small to determine reliable numbers by this method. As mentioned above several times, the chosen solvents had clear impacts on whether catenation occurred or not. Therefore, we looked at the van't Hoff-plots of temperature dependent ^{1}H NMR measurements of the equilibria **2 OMe-cube ↔ (OMe-cube)$_2$** and **2 SMe-cube ↔ (SMe-cube)$_2$** to get further insights whether the processes of catenation are enthalpy or entropy driven reactions. In both investigated cases the catenation is an entropy-driven reaction (ΔS_{OMe} = +114.3 J·K^{-1}mol^{-1} and ΔS_{SMe} = +185.3 J·K^{-1}mol^{-1}), rather than an enthalpically driven reaction (ΔHOMe = +13.1 kJ·mol^{-1} and ΔHSMe = +29.4 kJ·mol^{-1}), which also explains the temperature-dependency of the reaction. It further suggests that solvophobic effects[48] are dominating the catenation process at least in the investigated solvent systems. These solvophobic effects are dependent on polarity of side-chains,[49,50] as it is here the case and need to be investigated further for such systems.

Conclusions

We observed the formation of dimeric and trimeric cage catenane based on the weak interactions of the substituents of the constituent1,4-benzene dialdehydes. Whereas π-stacking as driving force was ruled out, Keesom and London dispersion interactions between the substituents as well as with the solvent were considered. Changing the methoxy groups to less polar ethyl groups decreased catenane formation significantly. In cases where there is only a methyl- or no substituent at the dialdehyde, the intermolecular forces are too weak to foster catenane formation. Finally, dialdehydes with thiomethyl substituents were beneficial to catenane formation and indeed a clear reaction to **(SMe-cube)$_2$** was observed, having

a difference of |ΔG°| of approx. 6 kJ/mol for catenane formation than the **(OMe-cube)$_2$**. Solvent effects play a crucial role in the cases where dimeric and trimeric catenation was observed. Both systems (with OMe and SMe substituents) showed the same trends. In TCE, monomeric cages **OMe-cube** and **SMe-cube** were formed selectively, whereas in dichlormethane at elevated temperatures the clean formation of trimeric catenanes **(OMe-cube)$_3$** and **(SMe-cube)$_3$** were observed. Comparing the coherence energy densities (ced's) of the solvents (TCE = 98.0 cal/cm^3 vs. DCM = 93.7 cal/cm^3) in combination of the data from van't Hoff plot analysis revealed, that solvophobic effects may play a major role, since reactions toward catenated cages are entropically favoured.

This motif of weak dispersion interactions in combination with solvophobic effects as driving force for catenation of shape-persistent organic cages allow to further study the influence of subtle structural changes in combination with chosen solvents as reaction media to understand events of dynamic covalent chemistry of larger and more complex structures as well as to construct e.g. poly[n]catenated cages with n > 3, e.g. for cages of higher molecular volumes.

Methods

Synthesis of (OMe-cube)$_2$

To a solution of TBTQ **1** (20 mg, 0.043 mmol) and 2,5-dimethoxy-terephthaldehyde **3** (12.6 mg, 0.0649 mmol) in deuterated chloroform (4 mL) in a screw-capped 8 mL glass vial, a catalytic amount of TFA (0.4 μL, 0.0052 mmol) was added and the reaction mixture was stirred at RT for 3 days. Afterwards, the crude reaction mixture was washed with aq. K2CO3 solution (0.25 M, 3 × 2 mL), dried over Na2SO4 and concentrated under reduced pressure. The resulting red colored solid was immediately dissolved in dichloromethane and purified by recycling gel permeation chromatography (r-GPC) (DCM, 35°C, 5 mL/min) to give 14 mg (46%) of **(OMe-cube)$_2$** as a yellow solid. **Mp**: 315°C (decomposed); ^{1}H NMR (600 MHz, CD_2Cl_2): δ = 8.90 (s, 6H, *H*C=N), 8.87 (s, 6H, *H*C=N), 8.85 (s, 12H, *H*C=N), 8.82 (s, 6H, *H*C=N), 8.78 (s, 6H, *H*C=N), 8.65 (s, 6H, *H*C=N), 8.38 (s, 6H, *H*C=N), 8.03 (s, 6H, Ar-*H*), 7.88 (s, 6H, Ar-*H*), 7.79 (s, 6H, Ar-*H*), 7.71 (s, 6H, Ar-*H*), 7.69 (12H, Ar-*H*), 7.53 (d, ^3J = 8.4 Hz, 6H, TBTQ Ar-*H*), 7.41 (d, ^3J = 8.4 Hz, 6H, TBTQ Ar-*H*), 7.38 (d, ^3J = 8.4 Hz, 6H, TBTQ Ar-*H*), 7.36-7.32 (m, 6H, TBTQ-Ar-*H* & Ar-*H*), 7.27 (s, 6H, TBTQ-Ar-*H*), 7.24 (s, 12H, Ar-*H*, TBTQ-Ar-*H*), 7.21 (s, 6H, TBTQ-Ar-*H*), 7.19 (s, 6H, TBTQ Ar-*H*), 7.17-7.14 (m, 6H, TBTQ-Ar-*H*), 7.08 (d, ^3J = 8.4 Hz, 6H, TBTQ-Ar-*H*), 7.03-6.97 (m, 18H, TBTQ-Ar-*H*), 6.89 (s, 6H, TBTQ-Ar-*H*), 6.83 (d, ^3J = 8.4 Hz, 6H, TBTQ-Ar-*H*), 6.78 (d, ^3J = 8.4 Hz, 6H, TBTQ-Ar-*H*), 6.77 (d, ^3J = 8.4 Hz, 6H, TBTQ-Ar-*H*), 6.72 (s, 6H, TBTQ-Ar-*H*), 6.59 (d, ^3J = 8.4 Hz, 12H, TBTQ-Ar-*H*), 6.26 (d, ^3J = 7.8 Hz, 6H, TBTQ-Ar-*H*), 4.04 (s, 18H, OC*H*$_3$), 3.94 (s, 18H, OC*H*$_3$), 3.90 (s, 18H, OC*H*$_3$), 3.86 (s, 18H, OC*H*$_3$), 3.82 (s, 18H, OC*H*$_3$), 3.67 (s, 18H, OC*H*$_3$), 3.11 (s, 18H, OC*H*$_3$), 2.85 (s, 18H, OC*H*$_3$), 2.30-1.74 (m, 96H, -C*H*$_2$CH$_2$CH$_3$) 1.71 (s, 30H), 1.64 (s, 18H), 1.35-1.09 (m, 84H, -CH$_2$C*H*$_2$CH$_3$), 1.0-0.90 (m, 126H, -CH$_2$CH$_2$C*H*$_3$), 0.77-0.72 (m, 12H, -CH$_2$C*H*$_2$CH$_3$), 0.48 (t, ^3J = 7.2 Hz, 18H, -C*H*$_2$CH$_2$*CH*$_3$); ^{13}C NMR (151 MHz, CD_2Cl_2): δ = 156.5, 155.7, 155.3, 155.2, 155.0, 154.6, 154.31, 154.26, 154.2, 153.9, 153.8, 153.1, 152.7, 152.5, 152.6, 152.3, 152.2, 150.1, 149.8, 149.64, 149.6, 149.5, 149.4, 149.3, 149.1, 146.7, 146.6, 146.4,

146.1, 146.0, 145.5, 145.4, 129.0, 128.9, 128.6, 128.55, 128.49, 127.8, 125.0, 124.6, 124.42, 124.36, 124.2, 124.0, 119.8, 119.7, 119.4, 119.04, 118.96, 118.8, 118.5, 118.4, 118.1, 117.5, 117.3, 116.1, 116.0, 111.2, 110.2, 109.83, 109.77, 109.63, 109.58, 73.5, 73.2, 73.0, 67.39, 67.35, 67.33, 67.23, 67.18, 66.9, 56.71, 56.68, 56.65, 56.61, 56.6, 56.4, 56.1, 55.4, 41.8, 41.2, 41.1, 41.0, 21.3, 21.1, 21.0, 20.9, 20.8, 20.3, 15.5, 15.4, 15.32, 15.29, 15.0, 14.9; **FT-IR** (neat, ATR): ν (cm^{-1}) = 2999 (w), 2957 (m), 2925 (m), 2870 (m), 2853 (m), 1734 (w), 1616 (m), 1593 (m), 1492 (s), 1482 (s), 1465 (s), 1410 (s), 1373 (m), 1211 (s), 1140 (m), 1043 (s), 974 (w), 882 (m), 821 (m), 701 (w); **UV/Vis** (CH_2Cl2): λmax (nm) = 296, 406; **MALDI-TOF** (DCTB): *m/z* $[M]^+$ calcd. for C752H768N48O48: 11245.94, found 11245.57. **Elemental analysis** calcd. for C752H768N48O48·33CH_2Cl2: C 67.11, H 5.98, N 4.79, found C 66.94, H 5.91, N 4.86.

Supplementary Material

Refer to Web version on PubMed Central for supplementary material.

Acknowledgements

The authors like to thank the European Research Council ERC in the frame of the consolidators grant CaTs n DOCs (grant no. 725765). We further would like to thank Dr. Julian Holstein (Universität Dortmund, Germany), Dr. Sven M. Elbert, Margit Brückner and Dr. Frank Rominger, (all Ruprecht-Karls-Universität Heidelberg) and Prof. Dieter Fenske (Karlsruhe Institute of Technology) for their efforts in getting single-crystal X-ray structures of the here described cages and catenanes. Support by the state of Baden-Württemberg through bwHPC and the German Research Foundation (DFG) through grant no INST 40/5751 FUGG (JUSTUS 2 cluster) is acknowledged.

Data availability

All data supporting the findings of this study are available within the paper and its Supporting Information. The original experimental data to this paper has been deposited in the repository heiDATA and can be downloaded via https://heidata.uni-heidelberg.de/privateurl.xhtml?token=96ab88cd-5fc2-4b2c-b836-522dab565ba2

References

1. Wasserman E. THE PREPARATION OF INTERLOCKING RINGS: A CATENANE1. J Am Chem Soc. 1960; 82: 4433–4434. DOI: 10.1021/ja01501a082
2. Forgan RS, Sauvage J-P, Stoddart JF. Chemical Topology: Complex Molecular Knots, Links, and Entanglements. Chem Rev. 2011; 111: 5434–5464. DOI: 10.1021/cr200034u [PubMed: 21692460]
3. Gil-Ramírez G, Leigh DA, Stephens AJ. Catenanes: Fifty Years of Molecular Links. Angew Chem Int Ed. 2015; 54: 6110–6150. DOI: 10.1002/anie.201411619
4. Erbas-Cakmak S, Leigh DA, McTernan CT, Nussbaumer AL. Artificial Molecular Machines. Chem Rev. 2015; 115: 10081–10206. DOI: 10.1021/acs.chemrev.5b00146 [PubMed: 26346838]
5. Kay ER, Leigh DA, Zerbetto F. Synthetic Molecular Motors and Mechanical Machines. Angew Chem Int Ed. 2007; 46: 72–191. DOI: 10.1002/anie.200504313
6. Dattler D, et al. Design of Collective Motions from Synthetic Molecular Switches, Rotors, and Motors. Chem Rev. 2020; 120: 310–433. DOI: 10.1021/acs.chemrev.9b00288 [PubMed: 31869214]
7. Schill G, Lüttringhaus A. The Preparation of Catena Compounds by Directed Synthesis. Angew Chem Int Ed. 1964; 3: 546–547. DOI: 10.1002/anie.196405461
8. Dietrich-Buchecker CO, Sauvage JP, Kintzinger JP. Une nouvelle famille de molecules: les metallo-catenanes. Tetrahedron Lett. 1983; 24: 5095–5098. DOI: 10.1016/S0040-4039(00)94050-4

9. Dietrich-Buchecker CO, Sauvage JP, Kern JM. Templated synthesis of interlocked macrocyclic ligands: the catenands. J Am Chem Soc. 1984; 106: 3043–3045. DOI: 10.1021/ja00322a055
10. Chichak KS, et al. Molecular Borromean Rings. Science. 2004; 304: 1308–1312. DOI: 10.1126/science.1096914 [PubMed: 15166376]
11. Ayme J-F, et al. A synthetic molecular pentafoil knot. Nat Chem. 2012; 4: 15–20. DOI: 10.1038/nchem.1193
12. Zhang L, et al. Stereoselective synthesis of a composite knot with nine crossings. Nat Chem. 2018; 10: 1083–1088. DOI: 10.1038/s41557-018-0124-6 [PubMed: 30202101]
13. Leigh DA, et al. Tying different knots in a molecular strand. Nature. 2020; 584: 562–568. DOI: 10.1038/s41586-020-2614-0 [PubMed: 32848222]
14. Leigh DA, et al. A molecular endless (74) knot. Nat Chem. 2021; 13: 117–122. DOI: 10.1038/s41557-020-00594-x [PubMed: 33318672]
15. Leigh DA, Pritchard RG, Stephens AJ. A Star of David catenane. Nat Chem. 2014; 6: 978–982. DOI: 10.1038/nchem.2056 [PubMed: 25343602]
16. Wu Q, et al. Poly[n]catenanes: Synthesis of molecular interlocked chains. Science. 2017; 358: 1434–1439. DOI: 10.1126/science.aap7675 [PubMed: 29192134]
17. Fujita M, Fujita N, Ogura K, Yamaguchi K. Spontaneous assembly of ten components into two interlocked, identical coordination cages. Nature. 1999; 400: 52–55. DOI: 10.1038/21861
18. Frank M, Johnstone MD, Clever GH. Interpenetrated Cage Structures. Chem Eur J. 2016; 22: 14104–14125. DOI: 10.1002/chem.201601752 [PubMed: 27417259]
19. Zhu R, et al. Catenation and Aggregation of Multi-Cavity Coordination Cages. Angew Chem Int Ed. 2018; 57: 13652–13656. DOI: 10.1002/anie.201806047
20. Bloch WM, Holstein JJ, Dittrich B, Hiller W, Clever GH. Hierarchical Assembly of an Interlocked M8L16 Container. Angew Chem Int Ed. 2018; 57: 5534–5538. DOI: 10.1002/anie.201800490
21. Ronson TK, Wang Y, Baldridge K, Siegel JS, Nitschke JR. An S10-Symmetric 5-Fold Interlocked [2]Catenane. J Am Chem Soc. 2020; 142: 10267–10272. DOI: 10.1021/jacs.0c03349 [PubMed: 32453562]
22. Wang L, Vysotsky MO, Bogdan A, Bolte M, Böhmer V. Multiple Catenanes Derived from Calix[4]arenes. Science. 2004; 304: 1312–1314. DOI: 10.1126/science.1096688 [PubMed: 15166377]
23. Li Y, et al. Sulfate anion templated synthesis of a triply interlocked capsule. Chem Commun. 2009; 7134–7136. DOI: 10.1039/B915548A
24. Hasell T, et al. Triply interlocked covalent organic cages. Nat Chem. 2010; 2: 750. doi: 10.1038/nchem.739 [PubMed: 20729895]
25. Zhang G, Presly O, White F, Oppel IM, Mastalerz M. A Shape-Persistent Quadruply Interlocked Giant Cage Catenane with Two Distinct Pores in the Solid State. Angew Chem Int Ed. 2014; 53: 5126–5130. DOI: 10.1002/anie.201400285
26. Zhang G, Presly O, White F, Oppel IM, Mastalerz M. A Permanent Mesoporous Organic Cage with an Exceptionally High Surface Area. Angew Chem Int Ed. 2014; 53: 1516–1520. DOI: 10.1002/anie.201308924
27. Wang Q, et al. Solution-Phase Dynamic Assembly of Permanently Interlocked Aryleneethynylene Cages through Alkyne Metathesis. Angew Chem Int Ed. 2015; 54: 7550–7554. DOI: 10.1002/anie.201501679
28. Li H, et al. Quantitative self-assembly of a purely organic three-dimensional catenane in water. Nat Chem. 2015; 7: 1003–1008. DOI: 10.1038/nchem.2392 [PubMed: 26587716]
29. Li P, et al. De Novo Construction of Catenanes with Dissymmetric Cages by Space-Discriminative Post-Assembly Modification. Angew Chem Int Ed. 2020; 59: 7113–7121. DOI: 10.1002/anie.202000442
30. Xu S, et al. Catenated Cages Mediated by Enthalpic Reaction Intermediates. CCS Chemistry. 0 doi: 10.31635/ccschem.020.202000360
31. Greenaway RL, et al. High-throughput discovery of organic cages and catenanes using computational screening fused with robotic synthesis. Nat Commun. 2018; 9 2849 doi: 10.1038/s41467-018-05271-9 [PubMed: 30030426]

32. Beaudoin D, Rominger F, Mastalerz M. Chiral Self-Sorting of [2+3] Salicylimine Cage Compounds. Angew Chem Int Ed. 2017; 56: 1244–1248. DOI: 10.1002/anie.201610782
33. Wagner P, et al. Chiral Self-sorting of Giant Cubic [8+12] Salicylimine Cage Compounds. Angew Chem Int Ed. 2021; 60: 8896–8904. DOI: 10.1002/anie.202016592
34. Xu D, Warmuth R. Edge-Directed Dynamic Covalent Synthesis of a Chiral Nanocube. J Am Chem Soc. 2008; 130: 7520–7521. DOI: 10.1021/ja800803c [PubMed: 18498163]
35. Beaudoin D, Rominger F, Mastalerz M. Synthesis and Chiral Resolution of C3-Symmetric Tribenzotriquinacenes. Eur J Org Chem. 2016; 2016: 4470–4472. DOI: 10.1002/ejoc.201600890
36. Beaudoin D, Rominger F, Mastalerz M. Chiral Self-Sorting of [2+3] Salicylimine Cage Compounds. Angew Chem. 2017; 129: 1264–1268. DOI: 10.1002/ange.201610782
37. Bhat AS, et al. Transformation of a [4+6] Salicylbisimine Cage to Chemically Robust Amide Cages. Angew Chem Int Ed. 2019; 58: 8819–8823. DOI: 10.1002/anie.201903631
38. Schneider MW, Oppel IM, Griffin A, Mastalerz M. Post-Modification of the Interior of Porous Shape-Persistent Organic Cage Compounds. Angew Chem Int Ed. 2013; 52: 3611–3615. DOI: 10.1002/anie.201208156
39. Schick THG, Rominger F, Mastalerz M. Examination of the Dynamic Covalent Chemistry of [2 + 3]-Imine Cages. J Org Chem. 2020; 85: 13757–13771. DOI: 10.1021/acs.joc.0c01887 [PubMed: 32933246]
40. Gilli G, Bellucci F, Ferretti V, Bertolasi V. Evidence for resonance-assisted hydrogen bonding from crystal-structure correlations on the enol form of the .beta.-diketone fragment. J Am Chem Soc. 1989; 111: 1023–1028. DOI: 10.1021/ja00185a035
41. Holsten M, et al. Soluble Congeners of Prior Insoluble Shape-Persistent Imine Cages. Chem-Eur J. 2021; 27: 9383–9390. DOI: 10.1002/chem.202100666 [PubMed: 33848032]
42. Dummy1
43. Ueberricke L, et al. Triptycene End-Capped Quinoxalinophenanthrophenazines (QPPs): Influence of Substituents and Conditions on Aggregation in the Solid State. Chem Eur J. 2019; 25: 11121–11134. DOI: 10.1002/chem.201902002 [PubMed: 31210369]
44. Wagner JP, Schreiner PR. London Dispersion in Molecular Chemistry—Reconsidering Steric Effects. Angew Chem Int Ed. 2015; 54: 12274–12296. DOI: 10.1002/anie.201503476
45. Hansch C, Leo A, Taft RW. A survey of Hammett substituent constants and resonance and field parameters. Chem Rev. 1991; 91: 165–195. DOI: 10.1021/cr00002a004
46. Charton M. Nature of the ortho effect. II. Composition of the Taft steric parameters. J Am Chem Soc. 1969; 91: 615–618. DOI: 10.1021/ja01031a016
47. Cavallo G, et al. The Halogen Bond. Chem Rev. 2016; 116: 2478–2601. DOI: 10.1021/acs.chemrev.5b00484 [PubMed: 26812185]
48. Garza AJ. Solvation Entropy Made Simple. Journal of Chemical Theory and Computation. 2019; 15: 3204–3214. DOI: 10.1021/acs.jctc.9b00214 [PubMed: 30912938]
49. Yang L, Adam C, Nichol GS, Cockroft SL. How much do van der Waals dispersion forces contribute to molecular recognition in solution. Nature Chemistry. 2013; 5: 1006–1010. DOI: 10.1038/nchem.1779
50. Yang L, Adam C, Cockroft SL. Quantifying Solvophobic Effects in Nonpolar Cohesive Interactions. Journal of the American Chemical Society. 2015; 137: 10084–10087. DOI: 10.1021/jacs.5b05736 [PubMed: 26159869]

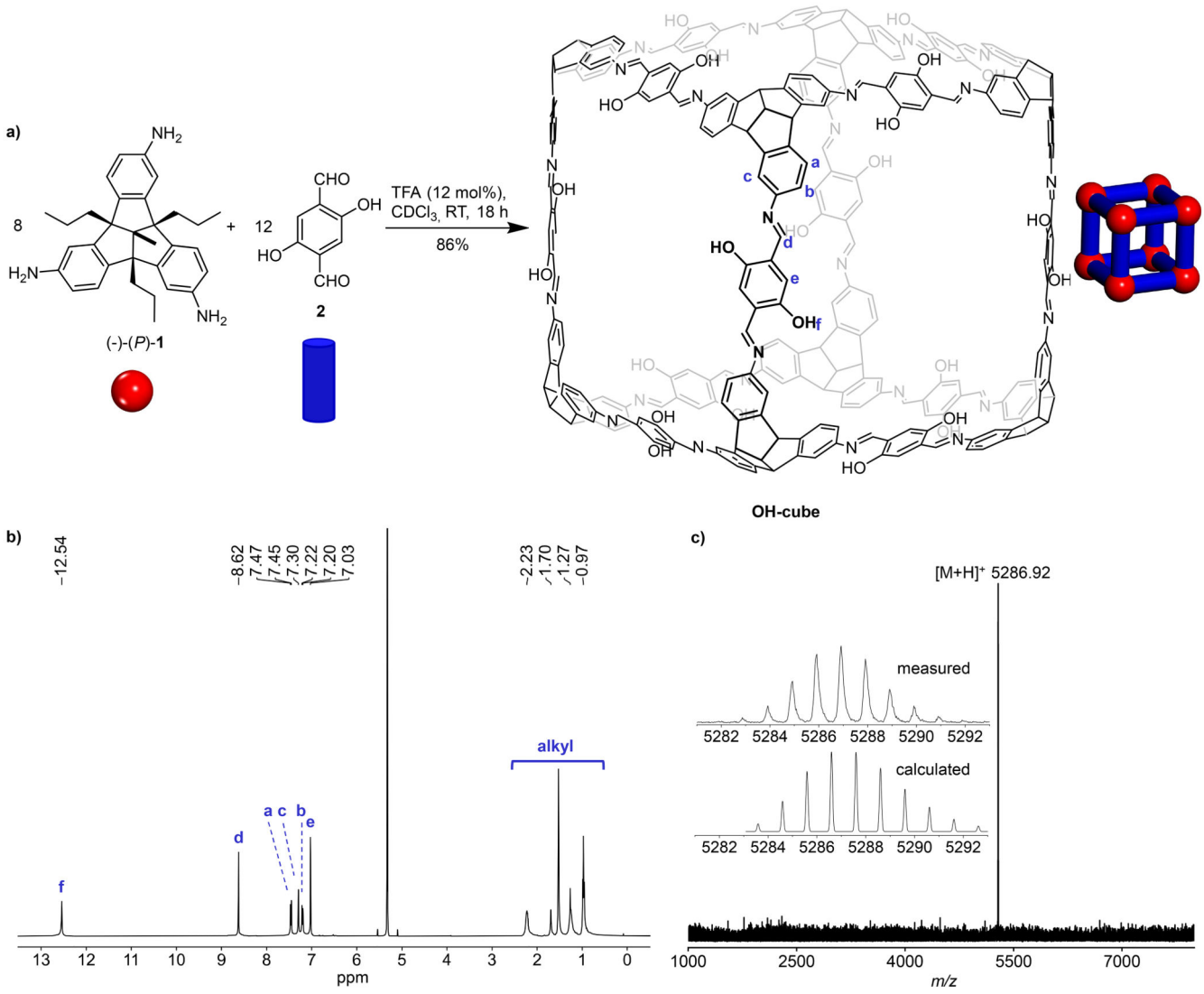

Figure 1. Synthesis and characterization of chiral OH-cube.

a Schematic representation of the acid catalysed 24-fold imine condensation of chiral TBTQ amine **1** and 2,5-dihydroxy terephthalaldehyde **2** to **OH-cube**. Please note that the alkyl substituents of TBTQ are omitted on the cubic structure of **OH-cube** for clarity. Reactants and cube are also drawn as cartoons. Red balls represent the TBTQ units and blue struts the aldehyde or imine linker units. **b** ^{1}H NMR spectrum (500 MHz, CD_2Cl_2, room temp.) of pure **OH-cube**. For assignment see atom labels in the molecular structure of **OH-cube** in panel a and Supplementary Section 2. **c** MALDI-TOF MS (DCTB) of pure **OH-cube**. The inset shows the comparison of measured and calculated isotopic patterns for **OH-cube**.

Europe PMC Funders Author Manuscripts

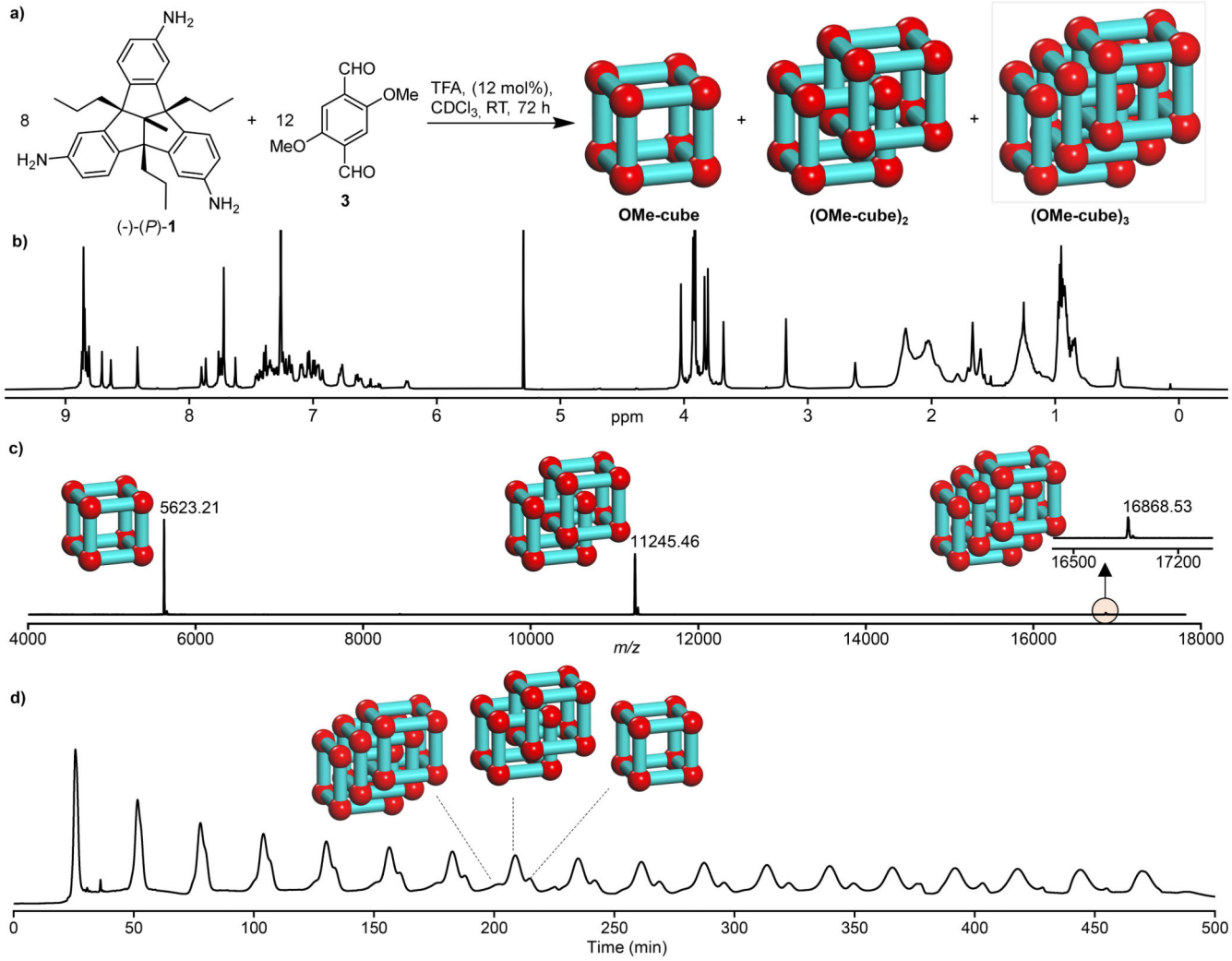

Figure 2. Synthesis and analysis of monomeric cage and dimeric and trimeric catenanes.

a Schematic representation of the acid catalysed 24-fold imine condensation of **1** and **2** to **OMe-cubes**. **b** and **c** ^{1}H NMR (600 MHz, $CDCl_3$) and MALDI-TOF MS (DCTB) of crude reaction mixture of **OMe-cubes**. ^{1}H NMR spectrum of the crude product was very complex but that the MALDI-TOF MS spectrum was relatively clear with three distinct peaks. Peaks in the MALDI-TOF MS are labelled with the structures of the products, and that the small peak for the trimeric catenane is highlighted and shown in inset. **d** r-GPC traces (solvent DCM) of the crude reaction mixture of **OMe-cube**, **(OMe-cube)$_2$ and (OMe-cube)$_3$** clearly show three peaks.

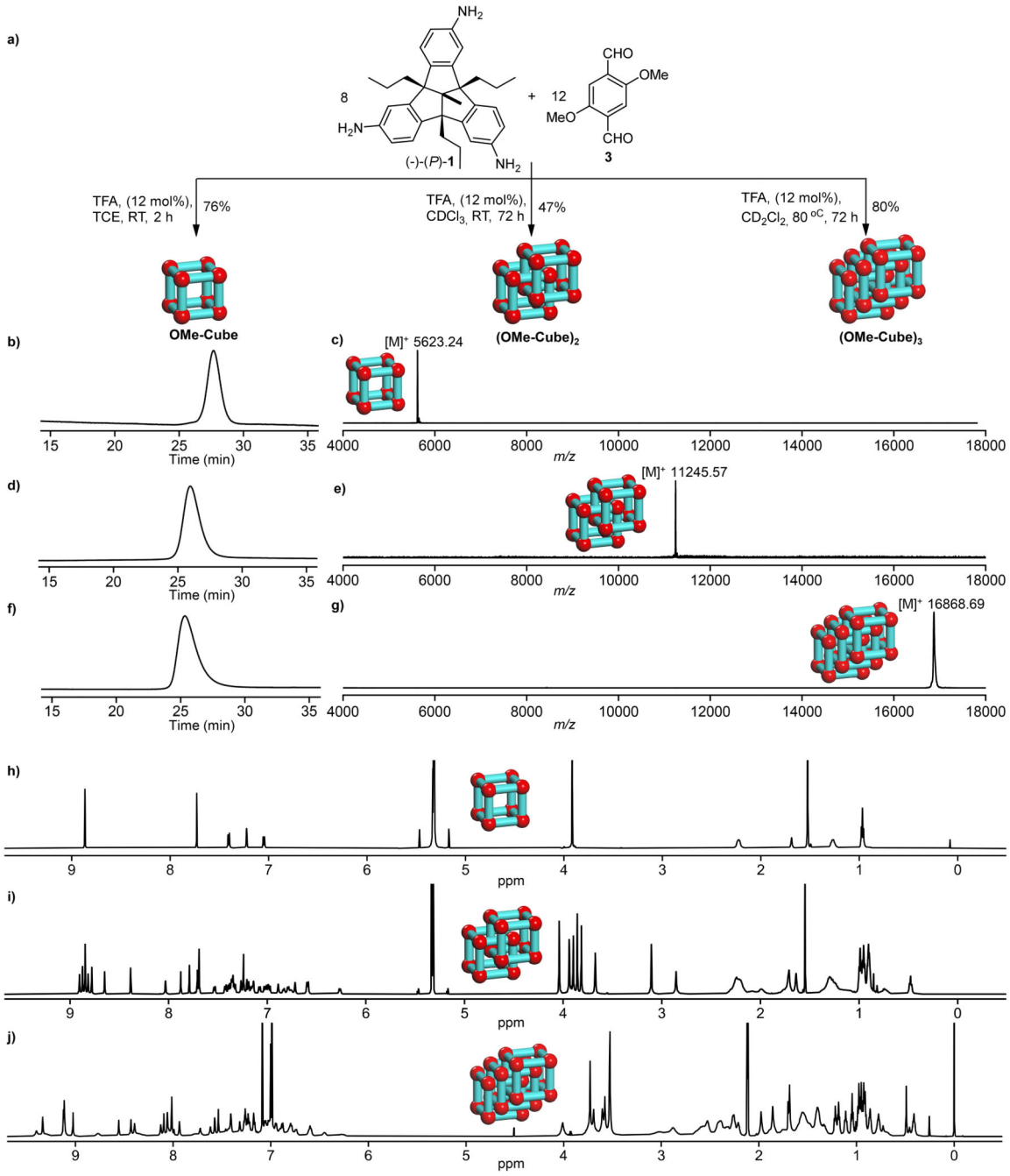

Figure 3. Selective synthesis and characterisation of OMe-cube, (OMe-cube)$_2$ and (OMe-cube)$_3$.

a Schematic representation of the acid catalysed 24-fold imine condensation of **1** and **3** in different solvents for the selective formation of **OMe-cube,** (**OMe-cube**)$_2$ and **(OMe-cube)$_3$**. For reaction details, see Supplementary Section 2. **b**, **d**, **f** r-GPC-traces (solvent DCM) of pure **OMe-cube,** (**OMe-cube**)$_2$ and **(OMe-cube)$_3$** show retention times 27.7, 25.9 and 25.4 minutes respectively which are consistent with their sizes. Depicted is the 1st cycle for each. **c**, **e**, **g** corresponding MALDI-TOF mass spectra of pure **OMe-cube,** (**OMe-cube**)$_2$ and **(OMe-cube)$_3$** showing exclusively single peak for each species**. h**, **i**, ^{1}H NMR spectra

(600MHz, 295 K, CD_2Cl_2) of pure **OMe-cube** and (**OMe-cube)$_2$. J** ^{1}H NMR spectra (700 MHz, 375 K, Toluene-d8) of pure **(OMe-cube)$_3$.**

Europe PMC Funders Author Manuscripts

Europe PMC Funders Author Manuscripts

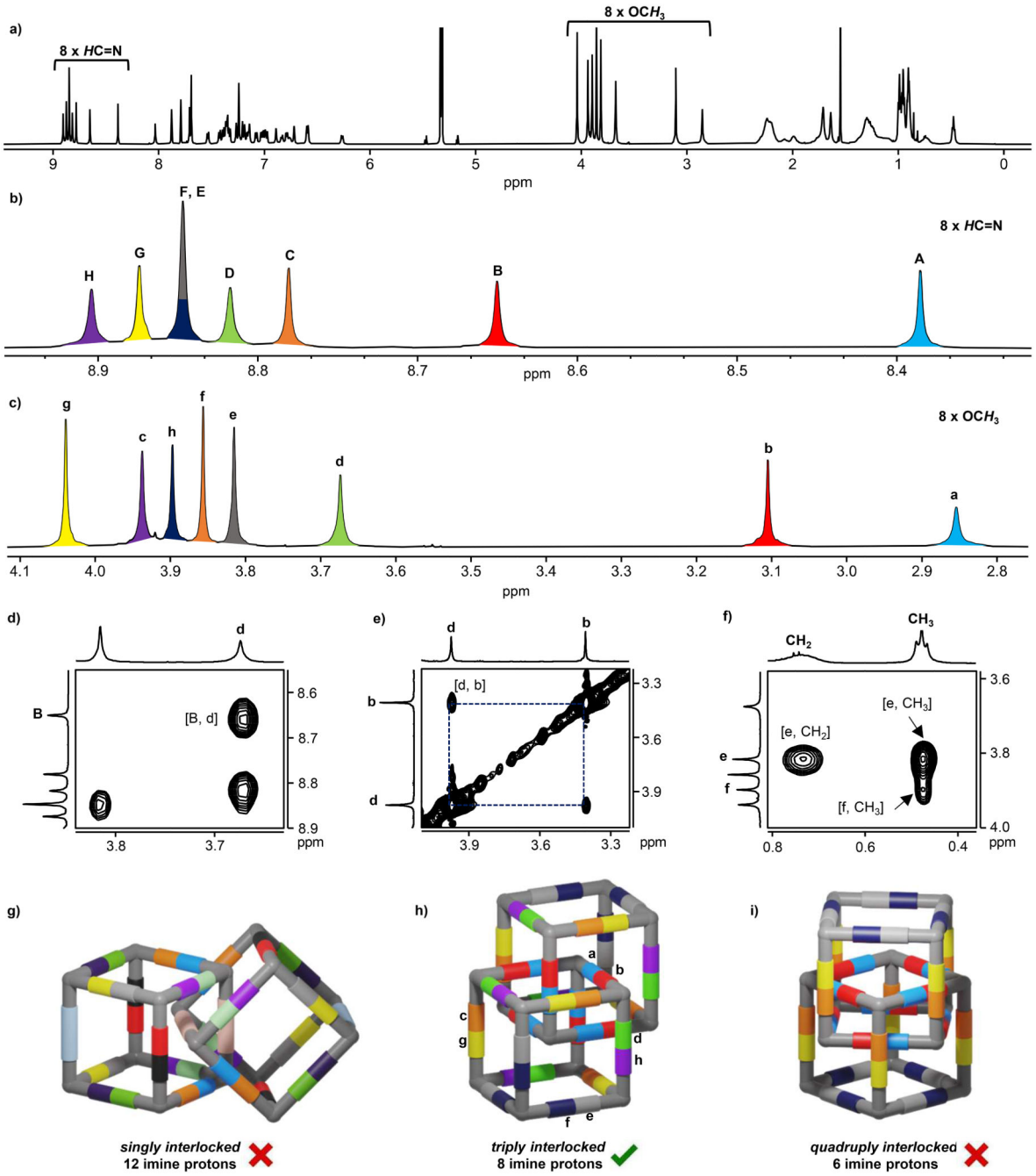

Figure 4. NMR spectroscopic analysis and assignment of (OMe-cube)$_2$.

a Full ^{1}H NMR (600 MHz, CD_2Cl_2) spectrum of (**OMe-cube**)$_2$. Partial ^{1}H NMR (600 MHz, CD_2Cl_2) showing eight different types of **b** imine peaks and **c** methoxy peaks of (**OMe-cube**)$_2$. **d** NOESY spectrum showing cross peaks between imine proton B and methoxy proton d. **e** NOESY spectrum showing cross peaks between methoxy protons b and d. **f** NOESY spectrum showing cross peaks between highly shielded aliphatic protons of propyl chains and methoxy protons e and f. **g** cartoon of the singly catenated cubes highlighting the 12 different magnetically equivalent imine protons respectively. **h** cartoon

of the triply interlocked catenated cube highlighting the 8 different magnetically equivalent imine protons. The colour code and assignment are the same as in **b** and **c**. **i** cartoons of the quadruply interlocked catenated cubes highlighting the 6 different magnetically equivalent imine protons respectively.

Europe PMC Funders Author Manuscripts

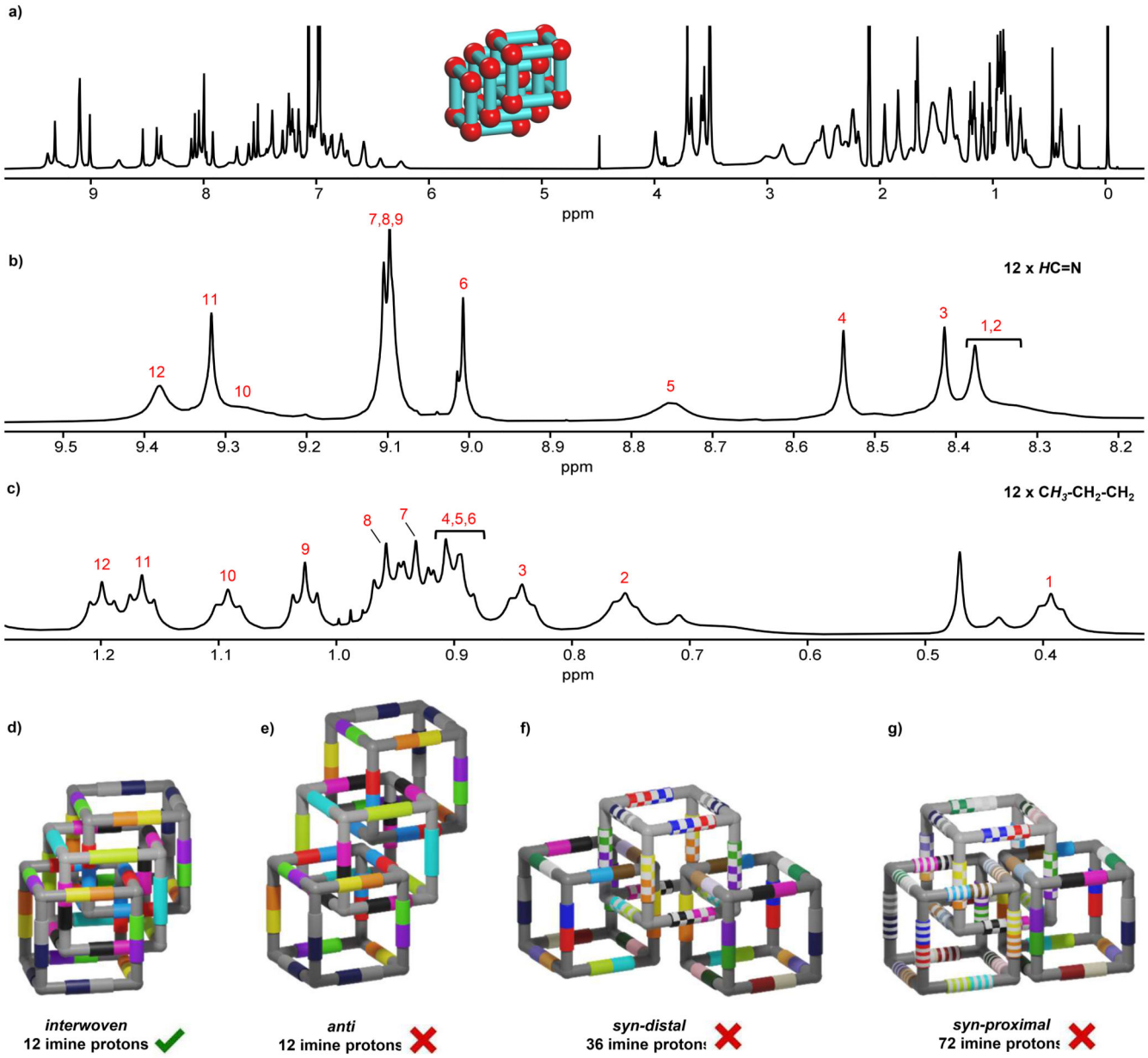

Figure 5. NMR spectroscopic analysis and assignment of (OMe-cube)$_3$.

a Full ^{1}H NMR (700 MHz, 375 K, Toluene-d$_8$) spectrum of (**OMe-cube)$_3$**. Partial ^{1}H NMR (700 MHz, 375 K, Toluene-d$_8$) showing twelve different types of **b** imine peaks and **c** methyl peaks of (**OMe-cube)$_3$**. Cartoons of the **d [(OMe-cube)@(OMe-cube)]@(OMe-cube), e (OMe-cube)@(OMe-cube)@(OMe-cube), f syn-distal** and **g syn-proximal trimeric catenanes** highlighting the 12, 12, 36 and 72 different magnetically equivalent imine protons in different colour codes respectively.

Europe PMC Funders Author Manuscripts

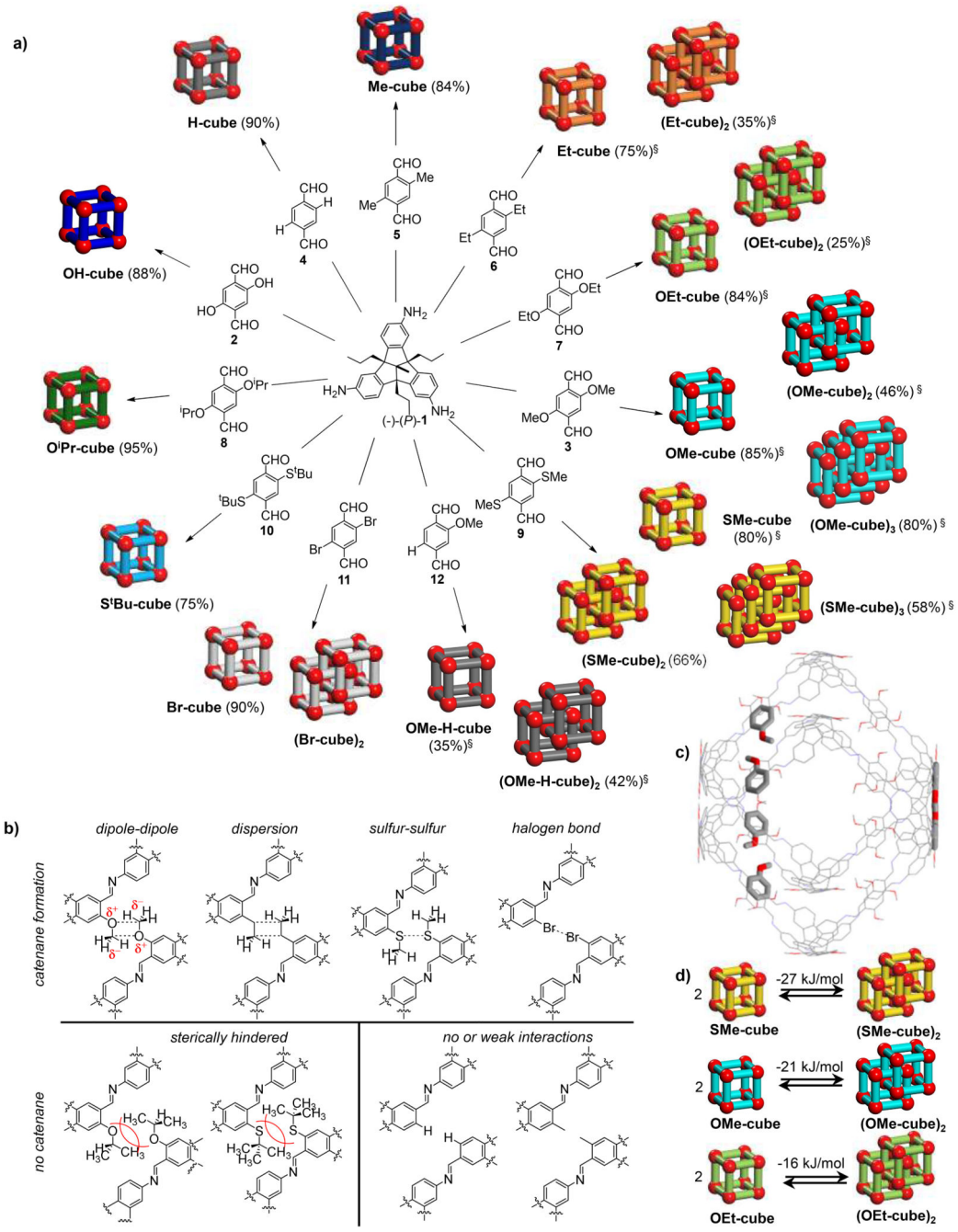

Figure 6. Summary of cage and catenanes with twelve different dialdehyde linkers.

a Reactions of various dialdehydes with TBTQ triamine **1**, giving cages (left side) or catenated cages (right side). **b** Summary of interactions resulting in catenane formation or their exclusion. **c** Possible conformational arrangement of the two interlocked cages with spatial arrangement of methoxy groups interacting via weak dipole–dipole forces (green dotted lines). **d** Gibb's enthalpy for catenation events determined by NMR spectroscopy. §Yields are given for optimized reactions.